Nanoscale

Accepted Manuscript

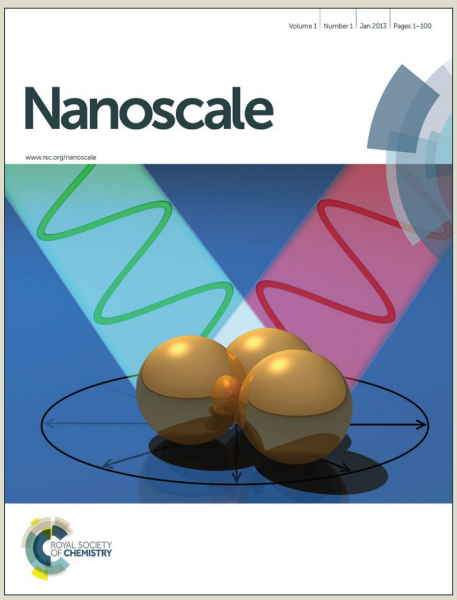

ROYAL SOCIETY OF CHEMISTRY

www.rsc.org/nanoscale

Silver nanoparticles impede phorbol myristate acetate-induced monocyte-macrophage differentiation and autophagy

Received 24th June 2015,
Accepted 00th January 20xx

DOI: 10.1039/x0xx00000x

www.rsc.org/

Yingying Xu,[a] Liming Wang,[a] Ru, Bai,[a] Tianlu Zhang,[a] Chunying Chen*[a]

Monocytes/macrophages are important constituent of the innate immune system. Monocyte-macrophage differentiation is not only crucial for the innate immune responses, but also related to some cardiovascular diseases. Silver nanoparticles (AgNPs) are one of the most widely used nanomaterials due to their broad-spectrum antimicrobial properties. However, the effect of AgNPs on the functions of blood monocytes is scarcely reported. Here, we report the impedance effect of AgNPs on THP-1 monocytes differentiation, and this effect was mediated by autophagy blockade and lysosomal impairment. Firstly, AgNPs inhibit phorbol 12-myristate 13-acetate (PMA)-induced monocytes differentiation by down-regulating both expression of surface marker CD11b and response to lipopolysaccharide (LPS) stimulation. Secondly, autophagy is activated during PMA-induced THP-1 monocytes differentiation, and autophagy inhibitor chloroquine (CQ) can inhibit this process. Thirdly, AgNPs block the degradation of the autophagy substrate p62 and induce autophagosomes accumulation, which demonstrates the blockade of autophagic flux. Fourthly, lysosomal impairments including alkalization and decrease of lysosomal membrane stability were observed in AgNPs-treated THP-1 cells. In conclusion, we demonstrate that the impedance of monocyte-macrophage differentiation by AgNPs is mediated by autophagy blockade and lysosomal dysfunction. Our results suggest there is a crosstalk existing in different biological effects induced by AgNPs.

Introduction

The broad-spectrum antimicrobial properties of silver nanoparticles (AgNPs) make them one of the most widely used nanomaterials.[1,2] Besides the medical use such as catheters, implants and other materials to prevent infection,[3] AgNPs are also used in consumer products such as water and air purification, food production, cosmetics and clothing.[4,5] For the inevitable human exposure to AgNPs, investigation on the comprehensive health and toxicological information is primary important. The toxicology of AgNPs has been studied for decades.[6] Our previous research have revealed both *in vitro* and *in vivo* toxicity of AgNPs,[7,8] and elucidated the cellular signal pathway and chemical origin of their cytotoxicity.[9-11] However, the influence of AgNPs on the functions of blood immune cells is nevertheless scarce.

Macrophages mediate innate immune responses and contribute to adaptive immunity *via* antigen processing.[12] Tissue macrophages are produced by the differentiation of monocytes recruited from the blood. Circulating monocytes are short-lived and will undergo apoptotic cell death in the absence of differentiation.[13] Growth factors including GM-CSF and M-CSF,[14] as well as inflammatory stimuli such as phorbol-12-myristate-13-acetate (PMA) and 1,25-dihydroxyvitamin D3 (VD3) can activate the pro-survival pathways of monocytes and induce their differentiation into macrophages.[15] However, little is known about the molecular mechanisms of monocyte-macrophage differentiation. Recently, Yuk et al. reported that VD3, a commonly used monocytes differentiation activator, induced autophagy in human primary monocytes as well as monocytic THP-1 cells.[16] What's more, Zhang et al. found that induction of autophagy is essential for GM-CSF triggered monocyte-macrophage differentiation.[17] Therefore, induction of autophagy might be one of mechanisms for the differentiation of monocytes to macrophages.

Autophagy is the basic catabolic mechanism that plays important roles in the degradation of unnecessary or dysfunctional cellular components through the actions of lysosomes.[18] During autophagy, cytosol and organelles are sequestered within double-membrane vesicles named autophagosomes, which are then fused with lysosomes and degraded or recycled. The breakdown of cellular components can ensure cellular survival during starvation by maintaining cellular energy levels. The main functions of autophagy are cellular homeostasis, anti-aging, anti-microbial and development. During the past decades, the toxicological effects of nanomaterials in molecular, cellular and animal level have been extensively investigated,[19] and autophagy has been considered as emerging mechanism of nanomaterials' toxicity, since many kinds of nanomaterials were reported to affect autophagy process.[20] A battery of nanomaterials has been visualized within the double membrane of autophagosomes, including carbon black, gold-coated iron oxide, quantum dots, silica and gold nanoparticles.[20] For instance, gold nanoparticles have been reported to block autophagy flux with autophagosome accumulation through size-dependent nanoparticles uptake and lysosomal impairment.[21] However, quantum dots, fullerene and its derivatives, dendrimers, and neodymium oxides were found to induce autophagy, and nanoparticles were therefore defined as a novel class of autophagy activators.[22]

AgNPs can be transported to blood circulation and distributed to several main organs even by oral administration.[23] Blood immune cells are important constitute of the immune system and the process of monocyte-macrophage differentiation is not only crucial for the innate immune responses, but also related to some cardiovascular disease such as atherosclerosis.[24] Therefore, it is essential to assess the toxicological effects of AgNPs on blood

[a] *CAS Key Laboratory for Biomedical Effects of Nanomaterials and Nanosafety, National Center for Nanoscience and Technology of China, Beijing, 100190, China.*
Tel: +86 10 82545560; fax: +86 10 62656765
E-mail: chenchv@nanoctr.cn (C. Chen).

immune cells. Although there are many reports on the toxicity of AgNPs, the influence of AgNPs on the monocyte-macrophage differentiation has not been reported. Also, the effects of AgNPs on the autophagy flux have not been thoroughly studied. In this work, we investigated the influence of AgNPs on both the monocyte-macrophage differentiation and autophagy flux in THP-1 cells, and found a crosstalk among these different toxicological effects of AgNPs.

Experimental

AgNPs characterization

AgNPs were provided by Institute for Health and Consumer Protection (IHCP, one Joint Research Centre of European Commission located in Italy) for the project of European Commission seventh framework program. The morphology and particle sizes of the AgNPs were determined by transmission electron microscope (TEM, Tecnai T20, Japan). The UV-Vis absorption spectra were acquired from a Lambda 35 spectrometer (PE, USA). The hydrodynamic diameter and surface charges in aqueous solution were measured with dynamic light scattering (DLS, Zetasizer, Malven Nano ZS90).

Cell culture and co-incubation with nanoparticles

THP-1 monocyte cell line was obtained from the American Type Culture Collection (ATCC). Cells were cultured in RPMI 1640 (Gibco BRL, Grand Island, NY) supplemented with 10% FBS, 10 mM HEPES, 2 mM glutamine, 100 U/mL penicillin, and 100 mg/mL streptomycin, and maintained in a humidified atmosphere containing 5% CO_2 at 37^{o}C. THP-1 cells were induced to differentiation in RPMI 1640 containing 100 nM phorbol 12-myristate 13-acetate (PMA, Sigma-Aldrich). All of the AgNPs solutions were fresh prepared from stock solutions and sonicated for 5 min before addition to cell cultures.

Flow cytometry

Flow cytometric measurements was employed to investigate the cell surface marker CD11b. THP-1 cells were seeded in 24-well plate at a density of 3×10^5 cells/well in the presence of 100 nM PMA. After differentiation for 24 h, fresh medium containing AgNPs with different concentration (5, 10 μg/mL) was added and the cells were cultured for another 24 or 48 h. After treatment, cells were harvested and washed twice with FACS buffer. Ten μL of PE-labeled mouse antibodies specific for CD11b or the relative IgG1 isotypes (Biolegend, USA) were added to each tube, respectively. After 30 min on ice in the dark, cells were washed three times with FACS buffer and resuspended in 350 μL cold FACS buffer. Flow cytometry (FACS Calibur, BD Bioscience, USA) was employed to analyze the surface marker CD11b of each sample.

ELISA

THP-1 cells were seeded in 24-well plate at a density of 3×10^5 cells/well in the presence of 100 nM PMA. After differentiation for 24 h, fresh medium containing AgNPs with different concentration (5, 10 μg/mL) was added and the cells were cultured for another 24 or 48 h. The supernatant was collected for cytokine analysis. The cytokines TNF-α in the supernatants were determined using a commercial ELISA kit (eBioscience, USA).

Immunofluorescence staining

THP-1 cells were seeded on glass coverslips that were placed inside the 6-well plate (6×10^5 cells per well), and cells were differentiated to attach overnight. In the following day, cells were treated with AgNPs (5, 10 μg/mL) for 24 h. Then the cells were fixed with 4% formaldehyde and treated with 1% Triton X-100. After blocked in 5% goat serum in PBS for 30 min, cells were processed for immunofluorescence with a monocolonal antibody to LC3 (Novus, USA) and the following secondary antibody FITC conjugated goat anti-rabbit antibody (Dingguo, China). After washed with PBS, coverslips were mounted onto the glass slides and examined with laser confocal microscope using 63X oil-immersion objective lens (Olympus FV500, Tokyo, Japan) and processed using Olympus Fluoview FV1000 software.

Western blot

THP-1 cells were seeded in 60 mm dishes at a density of 4×10^6 cells/well in the presence of 100 nM PMA. After differentiation for 24 h, fresh medium containing AgNPs (5, 10 μg/mL) was added and the cells were cultured for another 24 or 48 h. Chloroquine (CQ, 20 μM) was used as positive control. Then the cells were lysed in radioimmunoprecipitation assay (RIPA) buffer (50 mM Tris-HCl, pH 8.0, 150 mM NaCl, 1% Nonidet P-40, 0.5% sodium deoxycholate, 0.1% SDS, 2 mM EDTA, 1 mM NaVO4, 10 mM NaF) containing complete protease inhibitor cocktail (Roche). Protein concentration was determined by the Bicinchoninic Acid (BCA) protein assay kit. Equal amount of protein for each sample was subjected to SDS-PAGE and then transferred to a nitrocellulose membrane. Membranes were blocked in PBST buffer (0.1% Tween 20 in 0.01 M PBS) containing 5% non-fat milk powder, and then incubated with anti-LC3 or anti-β-actin (Santa Cruz, USA) antibodies overnight at 4^{o}C. The membrane was then incubated with an appropriate HRP-conjugated secondary antibody for 1 h at room temperature, then washed and reacted with supersignal chemiluminescent substrate (Pierce, USA). Blots were scanned on a Typhoon Trio Variable Mode Imager and analyzed with Typhoon Scanner Control v5.0 (GE Healthcare, USA).

Transmission electron microscopy

Cells were seeded in 60 mm dishes at a density of 4×10^6 cells/well in the presence of 100 nM PMA. After differentiation for 24 h, fresh medium containing CQ (20 μM) or AgNPs (5, 10 μg/mL) was added and the cells were cultured for another 24 or 48 h. Then cells were washed and isolated by centrifugation, fixed immediately with 2.5% glutaraldehyde at 4^{o}C overnight. Samples were prepared for TEM according to standard procedures then viewed using a JEOL JEM-1400 electron microscope (JEOL, Tokyo, Japan).

Cell viability and morphology

THP-1 cells were plated into a 96-well plate at a density of 1×10^5 per well in the presence of 100 nM PMA and cultured overnight.

The cell viability was assayed by 2-(2-methoxy-4-nitrophenyl)-3-(4-nitrophenyl)- 5-(2,4-disulf-opheyl)-2H-tetrazolium monosodium salt (WST-8), using Cell Counting Kit-8 (CCK-8, Dojindo Laboratories, Japan). AgNPs were introduced to the cells at the concentrations of 1, 5, 10 μg/mL, respectively. The cells cultured in the blank medium were taken as the control. After 24 h incubation, 10 μL CCK-8 solution was added to each well, followed by incubation for another 2.5 h. The OD of each well at 450 nm was measured with a microplate reader (Tecan Infinite M200, Swiss).

Lysosomal acidity and stability assay

THP-1 cells were seeded in 24-well plate at a density of 3×10^5 cells/well in the presence of 100 nM PMA. After differentiation for 24 h, fresh medium containing CQ (20 μM) or AgNPs (5, 10 μg/mL) was added and the cells were cultured for another 24 h. For lysosomal acidity assay, cells were washed twice with PBS and then incubated for 30 min with 500 μL of pre-warmed medium containing 2 μM LysoSensor Green DND-189 dye (Life Technologies, USA). After washing, fresh medium was added and the cells were observed using an Olympus IX71 fluorescence microscope (Tokyo, Japan). After trypsinization, the cells were resuspended in FACS buffer and immediately analyzed by flow cytometry. For lysosomal stability assay, cells were washed twice and then incubated with 5 μg/mL AO (Sigma, USA) for 15 min. After trypsinization, the cells were resuspended in FACS buffer and red fluorescence was analyzed by flow cytometry.

Statistics

At least three parallel experiments were conducted for each sample. The data were processed by Origin 8.0. Results were expressed as mean ± standard deviations (SD). Means of each treated group were statistically compared using the two-tailed Student's t-test. $p<0.05$ was considered statistically significant.

Results and discussion

THP-1 monocyte-macrophage differentiation induced by PMA

The differentiation of THP-1 monocytes was evaluated by the expression of surface marker CD11b and their response to LPS stimulation. CD11b is a characteristic marker expressed in macrophages while not in monocytes.[25] After treatment with PMA, the expression of CD11b in THP-1 cells increases significantly along with the incubation time, which is shown in Fig. 1A and 1B.

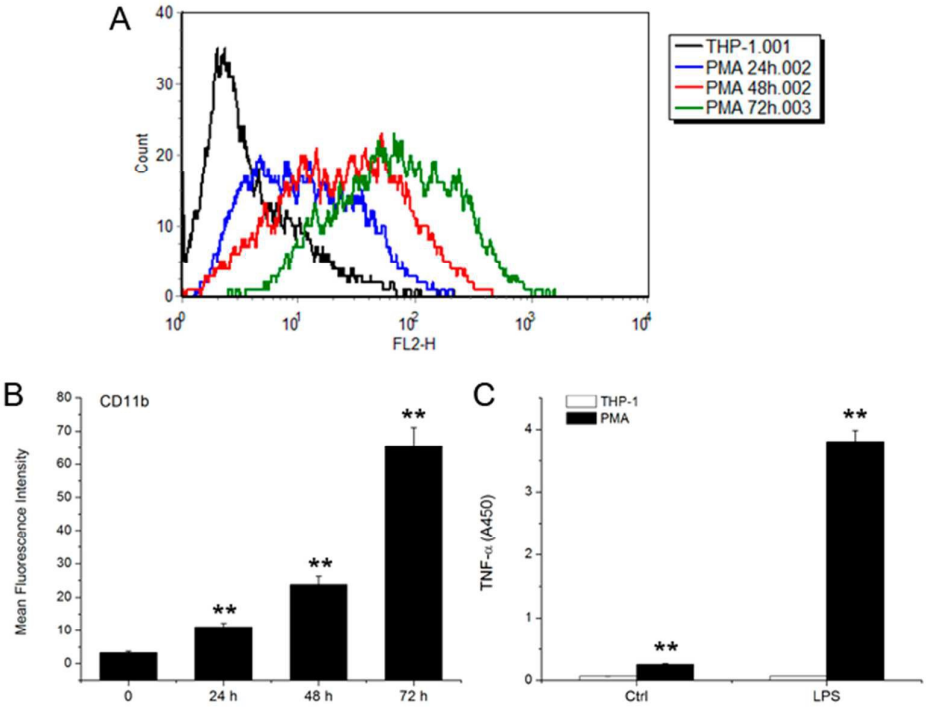

Fig.1 THP-1 monocytes differentiation induced by PMA. (A) Flow cytometry analysis of CD11b expression in THP-1 cells treated with PMA (100 nM) for different times; (B) Mean fluorescence intensity of CD11b expression in THP-1 cells treated with PMA (100 nM) for different times; (C) TNF-α secretion to LPS stimulation in THP-1 cells pretreated with or without PMA. $^{**}p < 0.01$ compared to control group.

Functionally, differentiated THP-1 can further be activated by LPS stimulation and secret inflammatory cytokine TNF-α. We detected the secretion of TNF- α with LPS stimulation in THP-1 cells with or without PMA treatment. As shown in Fig. 1C, the secretion of TNF-α by THP-1 monocytes is negligible even with LPS stimulation. Whereas, differentiated THP-1 cells induced by PMA treatment dramatically increase the secretion of TNF- α in especially with LPS stimulation. The up-regulated expression of surface marker CD11b

and increased secretion of TNF-α both demonstrate differentiation of THP-1 monocytes to macrophages.

Autophagy is activated during PMA-induced monocytes differentiation

To explore the role of autophagy in monocyte differentiation, we examined whether autophagy is activated in response to PMA treatment. THP-1 cells were treated with PMA to induce monocytes differentiation. Microtubule-associated protein light chain 3 (LC3) was used as a marker for the induction of autophagy. During autophagy, cytosolic LC3 (LC3-I) is converted to membrane-bound form (LC3-II) which accumulates on the autophagosome membrane and appears as puncta.[26] To determine the proportion of LC3-II form, we performed immunoblot analyses of LC3-I and LC3-II in THP-1 cells. Increased expression of LC3-II was observed in THP-1 cells after treatment with PMA for 24 h (Fig. 2A). LC3 aggregates were also observed in THP-1 cells after treatment with PMA for 24 h, as shown in Fig. 2B. Moreover, we obtained evidence for PMA-induced autophagy from electron microscopy, which revealed the presence of multiple autophagosome-like vacuoles with double-membrane structures (Fig. 2C). To investigate the effect of autophagy on the differentiation of monocytes, we detected the expression of characteristic macrophage marker CD11b in cells treated with an autophagy inhibitor CQ. Results shown in Fig. 2D indicated that CQ significantly inhibits the expression of CD11b in PMA-treated THP-1 cells. These results

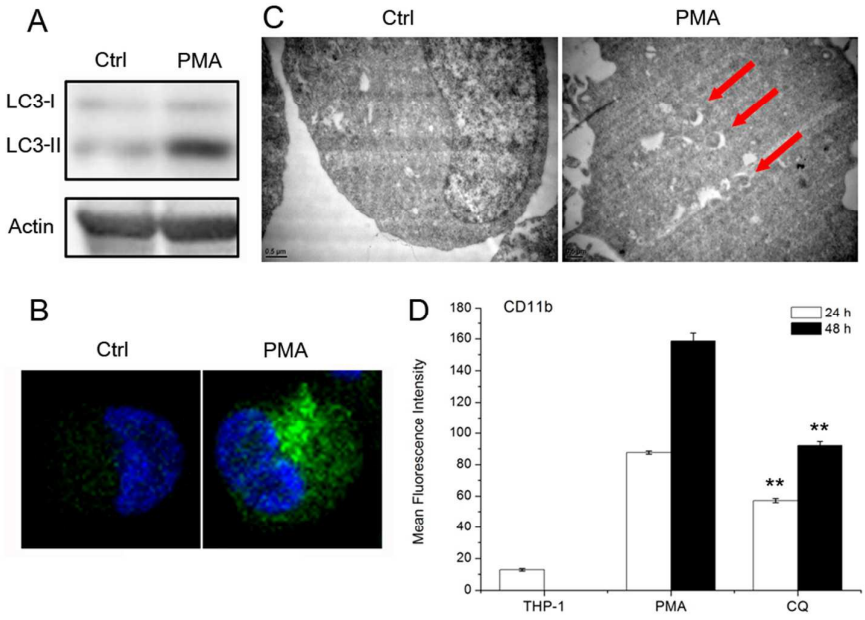

Fig. 2 Autophagy is activated during PMA-induced THP-1 monocytes differentiation. (A) Western blot analysis with anti-LC3 antibody for THP-1 monocytes incubated with or without PMA (100 nM) for 24 h; (B) Immunofluorescent images of LC3 in THP-1 monocytes treated with or without PMA (100 nM) for 24 h; (C) Transmission electron microscopy assay for THP-1 monocytes incubated with or without PMA (100 nM) for 24 h. Red arrows indicate autophagosomes with double membranes. Scale bars indicate 0.5 μm; (D) Expression of CD11b on THP-1 cells treated with PMA or PMA plus the autophagy inhibitor chloroquine (CQ, 20 μM) for the indicated times. $^{**}p < 0.01$ compared to PMA group.

suggest that autophagy is activated for PMA-induced monocytes differentiation, and the differentiation is impeded when autophagy process is blocked. Monocytes and macrophages are chief participants in host inflammatory responses. Deregulation of monocyte-macrophage differentiation may lead to some immune diseases. However, the molecular processes of monocyte-macrophage differentiation are not completely understood yet. Recently, Zhang et al. revealed that autophagy is activated during GM-CSF triggered human monocyte-macrophage differentiation.[17] However, whether autophagy is activated during PMA-induced monocytes differentiation has not been reported. Our present results demonstrate that autophagy is also activated for PMA-induced monocytes differentiation. The increased LC3 aggregates, elevated conversion of LC3-I to LC3-II, as well as the increased autophagosomes in the cytosol all illustrate the autophagy activation during the differentiation of THP-1 cells. The autophagy inhibitor CQ significantly inhibits the differentiation of THP-1 cells, which suggests that autophagy is essential for PMA-induced monocyte differentiation.

Characterization of AgNPs

TEM images of AgNPs are shown in Fig. 3A. They are round or oval shape, and the size is less than 30 nm. As shown in UV-Vis spectra (Fig. 3B), AgNPs exhibit specific absorption at 410 nm due to the surface plasmon resonance of AgNPs. The hydrodynamic diameter and zeta potential of AgNPs determined by dynamic light scattering in pure water was 38 nm and -4.3 mV, respectively.[9,11]

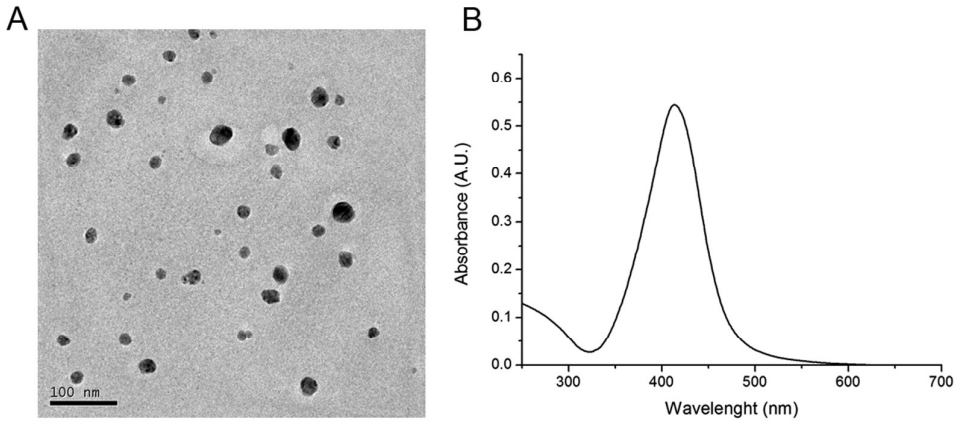

Fig. 3 Characterization of AgNPs. (A) TEM image of AgNPs. (B) UV-Vis absorption spectrum of AgNPs suspended in ultrapure water.

Inhibition of PMA-induced monocyte-macrophage differentiation by AgNPs

To investigate the effects of AgNPs on PMA-induced monocyte-macrophage differentiation, we assayed the expression of surface marker CD11b as well as the TNF- α secretion of THP-1 cells. After treatment with PMA to induce differentiation for 24 h, cells were further incubated with AgNPs for 24 or 48 h. As shown in Fig. 4A, AgNPs treatment significantly inhibits the expression of CD11b, and the inhibition effect increases along with the incubation time as well as the concentration of AgNPs. AgNPs can stimulate the TNF-α secretion without LPS, however, this stimulation effect convert to inhibition effect when LPS exist (Fig. 4B). These results indicate that AgNPs treatment decrease the response of PMA-induced macrophages to LPS stimulation. Silver ions (Ag^+) have the similar effects on the inhibition of CD11b expression and the TNF-α secretion with LPS stimulation, which indicate the inhibition effects of AgNPs are partially due to the existence of Ag^+. The present study demonstrates significant inhibition effects of AgNPs on the differentiation of THP-1 monocytes, which are illustrated by the down-regulated expression of surface marker CD11b and response to LPS stimulation.

Effects of AgNPs on the proliferation of THP-1 macrophages

Since differentiated THP-1 cells stop proliferation, we assayed the cells proliferation after treatment with AgNPs. When differentiated THP-1 cells were further incubated with AgNPs for 24 or 48 h, cell viability increased with the increasing of AgNPs concentration (Fig. 5A). The cell viability decreases slightly in 10 μg/mL AgNPs compared to 5 μg/mL AgNPs treated cells at 48 h exposure (Fig. 5A), which might be the result of the toxicity of increased Ag^+ in 10

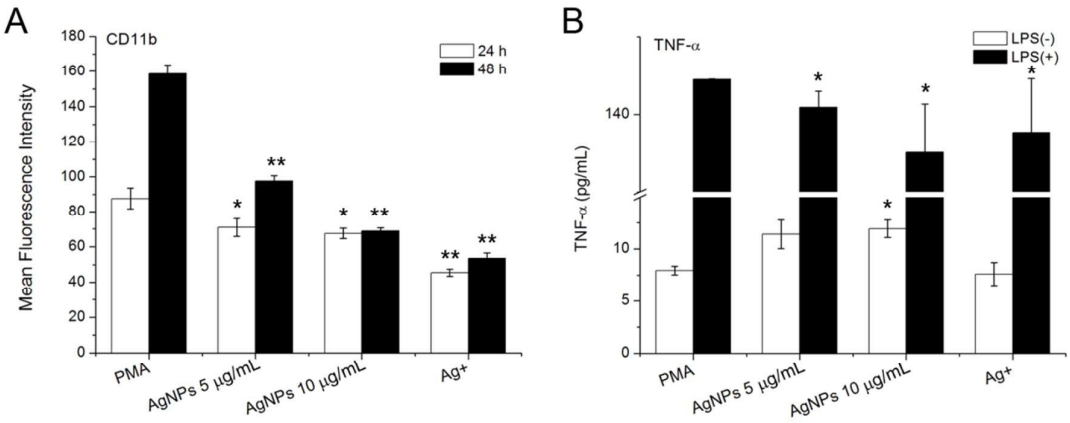

Fig. 4 Effects of AgNPs on PMA-induced THP-1 monocytes differentiation. (A) Effect of AgNPs on the CD11b expression on THP-1 cells treated by PMA and subsequent AgNPs (5, 10 μg/mL) or Ag^+ ($AgNO_3$, 1 μg/mL); (B) TNF-α secretion to LPS stimulation of THP-1 cells treated by PMA and subsequent AgNPs (5, 10 μg/mL) or Ag^+ ($AgNO_3$, 1 μg/mL). *$p < 0.05$, **$p < 0.01$ compared to only PMA-treated group.

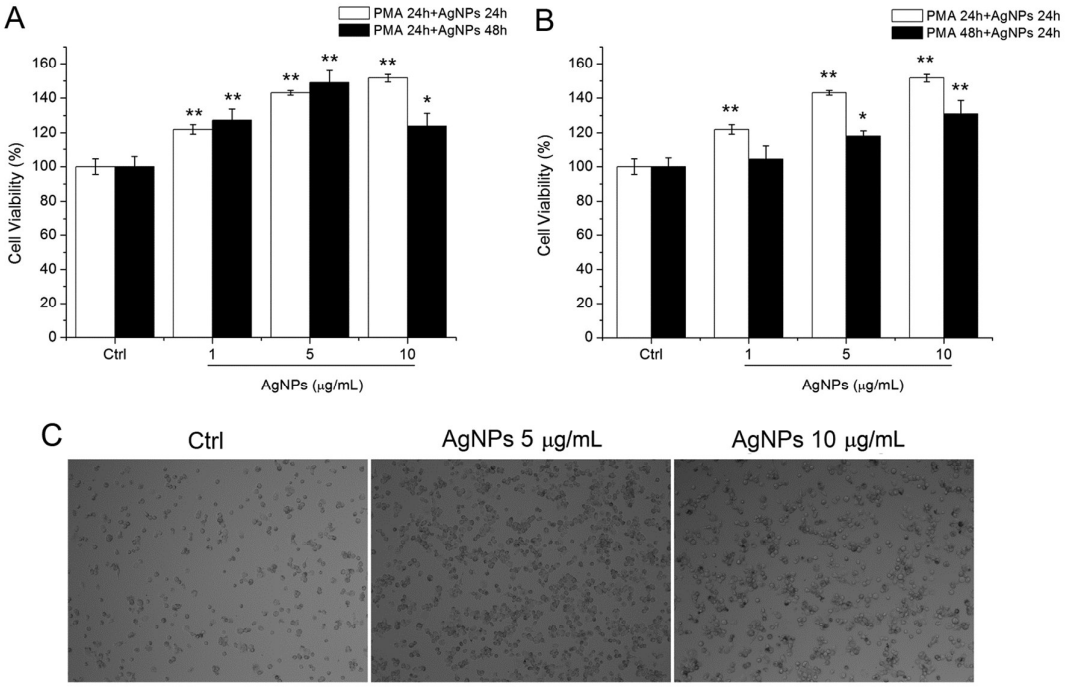

Fig. 5 Effects of AgNPs on the proliferation of THP-1 macrophages. (A) Cell viability of THP-1 cells treated first with PMA (100 nM) for 24 h and then with AgNPs (1, 5, 10 μg/mL) for 24 or 48 h; (B) Cell viability of THP-1 cells treated first with PMA (100 nM) for 24 h or 48 h and then with AgNPs (1, 5, 10 μg/mL) for 24 h; (C) Representative images of AgNPs treated THP-1 cells for 24 h photographed by an inverted phase contrast microscope (20× objective magnifications). *$p < 0.05$, **$p < 0.01$ compared to control group.

μg/mL AgNPs, since our previous study have demonstrated that the cytotoxicity mechanism of AgNPs was largely related to the intracellular release of Ag^+.[10,11] The extent of proliferation was also decreased when cells were first treated with PMA for 48 h, when the cells were more differentiated than cells treated with PMA for 24 h (Fig. 5B). Fig. 5C shows the phase-contrast images of control cells and cells treated with 5 and 10 μg/mL AgNPs for 48 h, which also demonstrates proliferation of AgNPs treated cells. The increased proliferation also demonstrates inhibition effect of AgNPs on the differentiation of THP-1 cells.

AgNPs triggers the formation of autophagosomes in THP-1 macrophages

To explore the mechanism for the inhibition effects of differentiation by AgNPs, we studied the impact of AgNPs on the process of autophagy activated by PMA, since autophagy is essential during monocytes differentiation. We examined the influence of AgNPs on the PMA-induced autophagy in THP-1 cells. Cells were first treated with PMA for 24 h to induce differentiation and autophagy, then the cells were incubated with AgNPs for 24 or 48 h. The conversion of LC3-I to LC3-II was assayed by western blot, and the results in Fig. 6A show that AgNPs treatment increases the proportion of LC3-II form. The increase is more significant in 10 μg/mL AgNPs treatment for 48 h. The lysosome-autophagosome fusion inhibitor CQ, which causes accumulation of LC3-II, was used as a positive control. TEM images show increased number of autophagosomes with double-membrane structures in AgNPs-treated cells compared to only PMA-treated cells (Fig. 6B and 2C). Additionally, a large number of empty vacuoles appear in the cytoplasm of AgNPs-treated cells. Immunofluorescence images also show that cells treated with AgNPs or CQ for 24 h increased LC3 aggregates compared to only PMA treated cells (Fig. 6C). These results demonstrate significant autophagosome accumulation in PMA-induced THP-1 macrophages by AgNPs treatment.

AgNPs blocks degradation of autophagy substrate p62

Autophagosome accumulation may be due to either autophagy induction or the blockade in downstream steps. “Autophagic flux” assays can help to distinguish between these two possibilities. We investigated the degradation of the autophagic substrate p62 in AgNPs-treated THP-1 monocytes. p62 is selectively incorporated into autophagosomes and effciently degraded by autophagy.[27] As shown in Fig. 7A, the p62 protein level was markedly increased after AgNPs treatment especially in 48 h. As CQ treatment, AgNPs

Nanoscale

ARTICLE

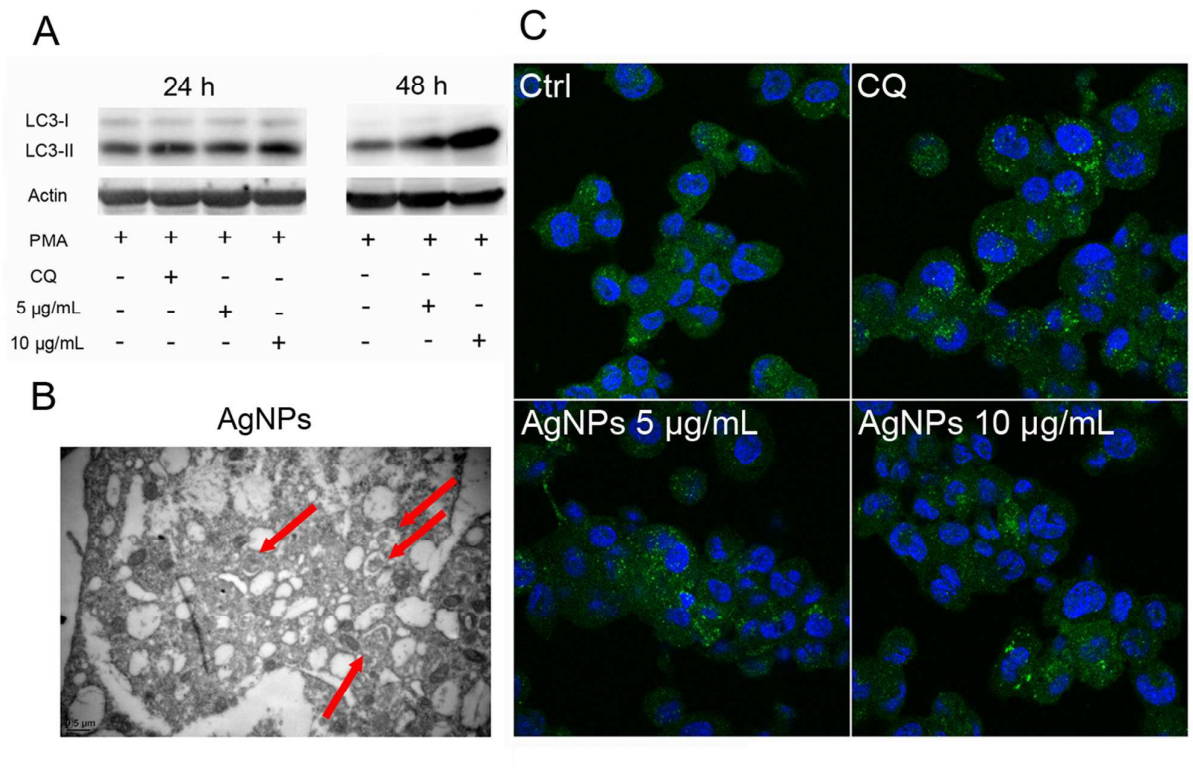

Fig. 6 Effects of AgNPs on the formation of autophagosomes in PMA treated THP-1 monocytes. (A) Western blot analysis with anti-LC3 antibody for THP-1 monocytes treated first with PMA (100 nM) for 24 h and then with AgNPs (5, 10 μg/mL) for 24 or 48 h. CQ (20 μM) was taken as a positive control; (B) TEM images of autophagosomes in THP-1 monocytes treated first with PMA (100 nM) for 24 h and then with AgNPs (5 μg/mL) for 24 h. Red arrows indicate autophagosomes with double membranes. Scale bars indicate 0.5 μm; (C) Immunofluorescent images of LC3 in THP-1 monocytes treated first with PMA for 24 h and then with AgNPs (5, 10 μg/mL) or CQ for 24 h.

treatment did not induce reduction in p62 level but instead caused accumulation of p62, which indicate possible impairment of autophagic degradation capacity (Fig. 7A). From the above results, we conclude that AgNPs treatment induce autophagosome accumulation through blockade of autophagic flux. Recently, Lee et al. reported the autophagic effects of AgNPs in mouse embryonic fibroblasts NIH 3T3 cells.[28] They observed the induced autophagosomes accumulation, the LC3 puncta formation and the expression of LC3-II protein. Although lysosomes were observed around the autophagosomes, autophagosomes did not merge with the lysosomes in the study. Therefore, it's unclear that if the observed autophagosome accumulation is due to autophagy activation or the blockade of autophagic flux. To elucidate that, we detected the degradation of the autophagic substrate p62 in AgNPs-treated THP-1 monocytes. Our results manifest that the degradation of p62 is blocked by AgNPs treatment, which suggests the blockade of autophagic flux. To conclude, AgNPs induce autophagosome accumulation by the blockade of autophagic flux, which further result in the inhibition of monocyte-macrophage differentiation.

Impairment of lysosome functions by AgNPs treatment

Lysosomes play an important role in autophagy process, which fuse with autophagosomes to form autolysosomes and then degrade the inner cellular components in the autolysosomes. Lysosomal dysfunction such as alkalization and lysosome membrane permeabilization may result in the blockade of autophagosome-lysosome fusion, as well as the accumulation of autophagosomes and autophagy substrates.[29] To determine whether AgNPs could interfere with lysosome function, the lysosomal pH and membrane

stability were assessed by using the LysoSensor Green DND-189 and acridine orange (AO), respectively. The LysoSensor dye is an acidotropic probe that accumulates in acidic organelles as the result of protonation. It exhibits a well-defined pH-dependent increase in

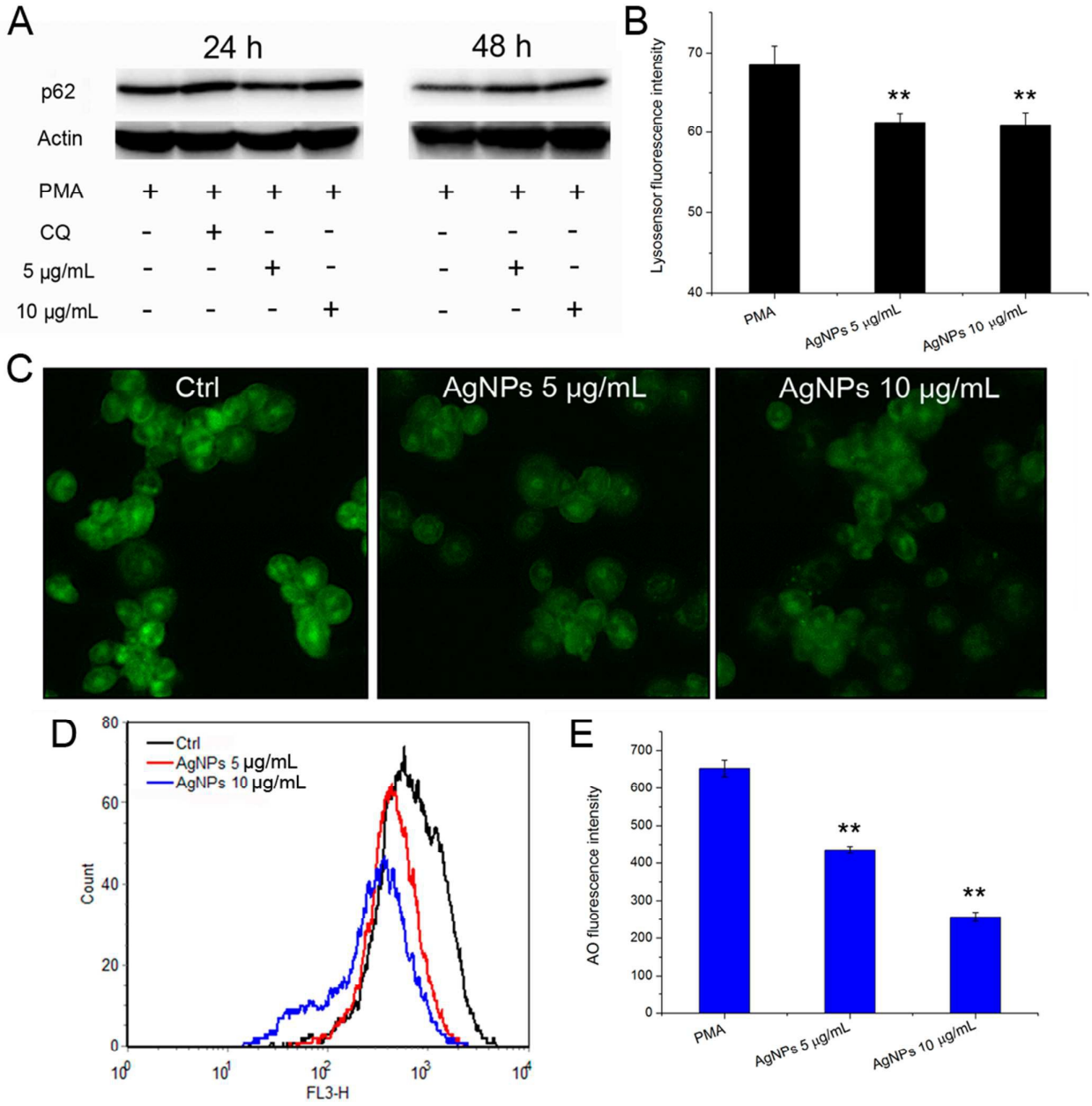

Fig. 7 Effects of AgNPs on the degradation of autophagy-specific substrate p62 and lysosomal functions. (A) Western blot analysis of autophagy-specific substrate p62 in THP-1 cells treated first with PMA (100 nM) for 24 h and then with AgNPs (5, 10 μg/mL) for 24 or 48 h. CQ (20 μM) was taken as a positive control; (B-C) Effect of AgNPs on lysosome pH. (B) Flow cytometry analysis of THP-1 cells treated first with PMA for 24 h and then with AgNPs for 24 h, then exposed for 30 min to 1 μmol/L LysoSensor Green DND-189; (C) Representative fluorescent images of cells stained with LysoSensor Green DND-189; (D-E) Effect of AgNPs on lysosome membrane stability. (D) Flow cytometry analysis of acridine orange (AO) in THP-1 cells treated first with PMA for 24 h and then with AgNPs (5, 10 μg/mL) for 24 h; (E) Mean fluorescence intensity of AO in THP-1 cells. $^{**}p < 0.01$ compared to control group.

Nanoscale

ARTICLE

fluorescence intensity upon acidification. Fluorescent microscopic analysis showed decrease of fluorescence signal in AgNPs-treated THP-1 cells (Fig. 7B). However, no obvious concentration effect was observed. Flow cytometry analysis confirmed this effect (Fig. 7C). These results demonstrate that AgNPs treatment causes alkalization of lysosomes.

AO can enter acidic compartments such as lysosomes and become protonated and emit orange fluorescence. Diminished fluorescence indicates the lysosomal leakage of AO and decrease of lysosomal membrane stability. The results in Fig. 7D and E indicate a significant decrease of lysosomal membrane stability in AgNPs-treated cells. The loss of lysosomal membrane stability is AgNPs

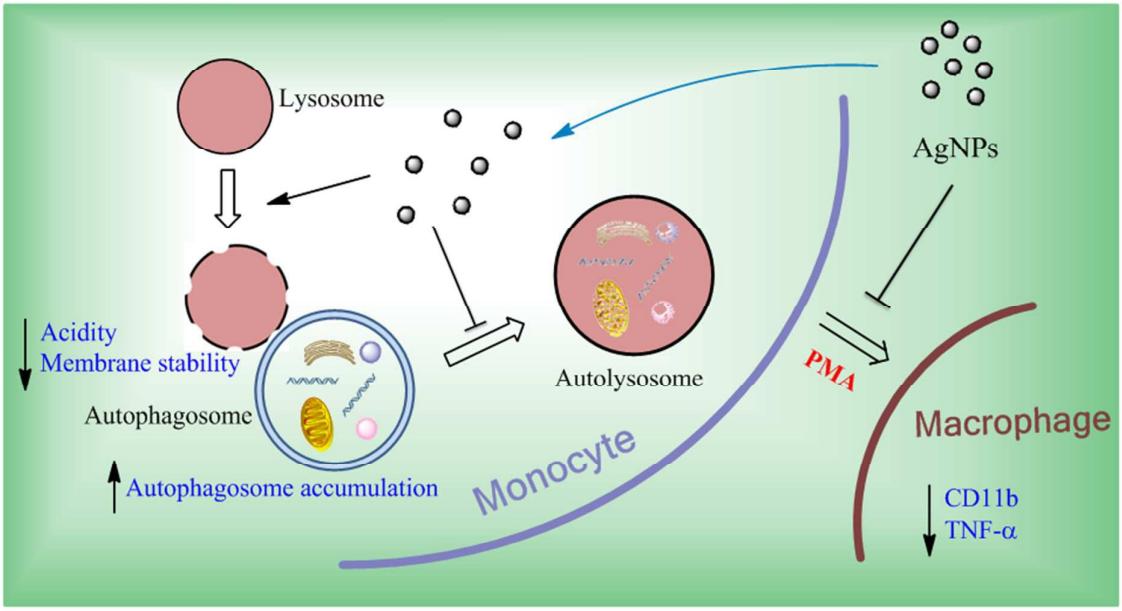

Fig. 8 Schematic illustration of the crosstalk among THP-1 monocytes differentiation, autophagy and lysosomal dysfunction simultaneously induced by AgNPs. The impedance of monocyte-macrophage differentiation by AgNPs is mediated by autophagy blockade and lysosomal dysfunction.

concentration-dependent. With the increase of the concentration of AgNPs, the lysosomal membrane stability decreases (Fig. 7D and E).

Our present results show the alkalization of lysosomes and decrease of the lysosomal membrane stability in AgNPs-treated THP-1 cells. Recently, lysosomal dysfunction has been considered as new mechanisms of nanomaterial toxicity. A great variety of nanomaterials have been reported to be associated with lysosomal dysfunction.[20] Lysosome alkalization can cause impairment of lysosome degradation capacity,[30] and lysosomal membrane permeabilization may result in mitochondrial outer membrane permeabilization and cellular apoptosis or necrosis.[31] Therefore, the lysosome impairment might be one mechanism for the decreased degradation capacity for p62 and the blockade of autophagic flux.

Conclusions

In the present study, we demonstrate that AgNPs impede PMA-induced monocyte-macrophage differentiation through autophagy blockade, which is further mediated by lysosomal dysfunction. We manifest that autophagy is an essential process for PMA-induced THP-1 monocytes differentiation, which is indicated by increased LC3 aggregates, elevated conversion of LC3-I to LC3-II, as well as increased autophagosomes in the cytosol. AgNPs inhibit THP-1 monocytes differentiation by down-regulating the expression of

surface marker CD11b and response to LPS stimulation. Autophagosomes accumulation and the blockade of the degradation of p62 were observed after AgNPs treatment, which demonstrates the blockade of autophagic flux. Furthermore, significant lysosomal impairment including alkalinization and decrease of the lysosomal membrane stability were observed in AgNPs-treated THP-1 cells, which is responsible for the blockade of autophagic flux. These results suggest a crosstalk among monocytes differentiation, autophagy and lysosomal dysfunction simultaneously induced by AgNPs. The exact molecular mechanisms for the crosstalk among these biological effects induced by AgNPs need further investigation.

Disclosures

The authors have no financial conflicts of interest.

Acknowledgements

We acknowledge the financial support from the National Basic Research Program of China (2011CB933400), the National Science Foundation of China (21320102003, 21403043), Beijing National Science Foundation (2152037) and the National Science Fund for Distinguished Young Scholars (11425520).

References

1 K. Chaloupka, Y. Malam, and A. M. Seifalian. *Trends Biotechnol*., 2010, 28, 580-588.
2 S. Shrivastava, T. Bera, A. Roy, G. Singh, P. Ramachandrarao, and D. Dash. *Nanotechnology*, 2007, 18,
3 M. Ahamed, M. S. AlSalhi, and M. K. J. Siddiqui. *Clin. Chim. Acta*, 2010, 411, 1841-1848.
4 T. M. Benn and P. Westerhoff. *Environ. Sci. Technol.*, 2008, 42, 7025-7026.
5 Q. Chaudhry, M. Scotter, J. Blackburn, B. Ross, A. Boxall, L. Castle, R. Aitken, and R. Watkins. *Food Addit. Contam. A,* 2008, 25, 241-258.
6 S. W. P. Wijnhoven, W. J. G. M. Peijnenburg, C. A. Herberts, W. I. Hagens, A. G. Oomen, E. H. W. Heugens, B. Roszek, J. Bisschops, I. Gosens, D. Van de Meent, S. Dekkers, W. H. De Jong, M. Van Zijverden, A. J. A. M. Sips, and R. E. Geertsma. *Nanotoxicology,* 2009, 3, 109-U78.
7 X. M. Jiang, R. Foldbjerg, T. Miclaus, L. M. Wang, R. Singh, Y. Hayashi, D. Sutherland, C.Y. Chen, H. Autrup, and C. Beer. *Toxicol. Lett*, 2013, 222: 55-63.
8 C. F. Pang, A. Brunelli, C. H. Zhu, D. Hristozov, Y. Liu, E. Semenzin, W. Wang, W. Q. Tao, J. N. Liang, A. Marcomini, C. Y. Chen, and B. Zhao. *Nanotoxicology*, 2015, DOI: 10.3109/17435390.2015.1024295.
9 L. L. Huo, R. Chen, L. Zhao, X. F. Shi, R. Bai, D. X. Long, F. Chen, Y. L. Zhao, Y.-Z. Chang, and C. Y. Chen. *Biomaterials*, 2015, 61, 307-315.
10 X. M. Jiang, T. Miclaus, L. M. Wang, R. Foldbjerg, D. Sutherland, H. Autrup, C. Y. Chen, and C. Beer. *Nanotoxicology,* 2015, 9, 181-189.
11 L. M. Wang, T. L. Zhang, P. Y. Li, W. X. Huang, J. L. Tang, P. Y. Wang, J. Liu, Q. X. Yuan, R. Bai, B. Li, K. Zhang, Y. L. Zhao, and C. Y. Chen. *ACS Nano*, 2015, 9, 6532-6547.
12 B. L. Burke, CE, *The Macrophage* 2002: Oxford University Press.
13 S. D. Ricardo, H. van Goor, and A. A. Eddy. *J. Clin. Invest.*, 2008, 118, 3522-3530.
14 P. A. Kiener, P. M. Davis, G. C. Starling, C. Mehlin, S. J. Klebanoff, J. A. Ledbetter, and W. C. Liles. *J. Exp. Med*., 1997, 185, 1511-1516.
15 E. K. Park, H. S. Jung, H. I. Yang, M. C. Yoo, C. Kim, and K. S. Kim. *Inflamm. Res.*, 2007, 56, 45-50.
16 J. M. Yuk, D. M. Shin, H. M. Lee, C. S. Yang, H. S. Jin, K. K. Kim, Z. W. Lee, S. H. Lee, J. M. Kim, and E. K. Jo. *Cell Host Microbe.*, 2009, 6, 231-243.
17 Y. Zhang, M. J. Morgan, K. Chen, S. Choksi, and Z. G. Liu. *Blood,* 2012, 119, 2895-2905.
18 F. Reggiori and D. J. Klionsky. Eukaryot. Cell, 2002, 1, 11-21.
19 A. Nel, T. Xia, L. Madler, and N. Li. *Science*, 2006, 311, 622-627.
20 S. T. Stern, P. P. Adiseshaiah, and R. M. Crist. *Part. Fibre Toxicol.,* 2012, 9,
21 X. W. Ma, Y. Y. Wu, S. B. Jin, Y. Tian, X. N. Zhang, Y. L. Zhao, L. Yu, and X. J. Liang. *ACS Nano*, 2011, 5, 8629-8639.
22 O. Zabirnyk, M. Yezhelyev, and O. Seleverstov. *Autophagy*, 2007, 3, 278-281.
23 K. Loeschner, N. Hadrup, K. Qvortrup, A. Larsen, X. Gao, U. Vogel, A. Mortensen, H. R. Lam, and E. H. Larsen. *Part. Fibre Toxicol*., 2011, 8, 18.
24 P. Shashkin, B. Dragulev, and K. Ley. *Curr. Pharm. Design,* 2005, 11, 3061-3072.
25 H. Schwende, E. Fitzke, P. Ambs, and P. Dieter. *J. Leukocyte Biol.*, 1996, 59, 555-561.
26 N. Mizushima, T. Yoshimori, and B. Levine. *Cell*, 2010, 140, 313-326.
27 G. Bjorkoy, T. Lamark, A. Brech, H. Outzen, M. Perander, A. Overvatn, H. Stenmark, and T. Johansen. *J. Cell Biol*., 2005, 171, 603-614.
28 Y. H. Lee, F. Y. Cheng, H. W. Chiu, J. C. Tsai, C. Y. Fang, C. W. Chen, and Y. J. Wang. *Biomaterials*, 2014, 35, 4706-4715.
29 N. Mizushima, B. Levine, A. M. Cuervo, and D. J. Klionsky. *Nature*, 2008, 451, 1069-1075.
30 K. A. Christensen, J. T. Myers, and J. A. Swanson. *J. Cell Sci.*, 2002, 115, 599-607.
31 B. Ravikumar, S. Sarkar, J. E. Davies, M. Futter, M. Garcia-Arencibia, Z. W. Green-Thompson, M. Jimenez-Sanchez, V. I. Korolchuk, M. Lichtenberg, S. Q. Luo, D. C. O. Massey, F. M. Menzies, K. Moreau, U. Narayanan, M. Renna, F. H. Siddiqi, B. R. Underwood, A. R. Winslow, and D. C. Rubinsztein. *Physiol. Rev*., 2010, 90, 1383-1435.